

# Developing a Warning System for Inbound Tsunamis from the Cascadia Subduction Zone

Randall J. LeVeque

*Applied Mathematics Department  
University of Washington  
Seattle, WA 98195-3925  
rjl@uw.edu*

Paul Bodin

*Department of Earth and Space Sciences  
University of Washington  
Seattle, WA 98195-3925  
bodin@uw.edu*

Geoffrey Cram

*Applied Physics Laboratory  
University of Washington  
Seattle, WA 98105-6698  
cramg@uw.edu*

Brendan W. Crowell

*Department of Earth and Space Sciences  
University of Washington  
Seattle, WA 98105-1310  
crowellb@uw.edu*

Frank I. González

*Department of Earth and Space Sciences  
University of Washington  
Seattle, WA 98195-3925  
figonzal@uw.edu*

Michael Harrington

*Applied Physics Laboratory  
University of Washington  
Seattle, WA 98105-6698  
mikeh@apl.washington.edu*

Dana Manalang

*Applied Physics Laboratory  
University of Washington  
Seattle, WA 98105-6698  
manalang@uw.edu*

Diego Melgar

*Department of Earth Sciences  
University of Oregon  
Eugene, OR 97405  
dmelgarm@uoregon.edu*

David A. Schmidt

*Department of Earth and Space Sciences  
University of Washington  
Seattle, WA 98195-3925  
dasc@uw.edu*

John E. Vidale

*Southern California Earthquake Center  
University of Southern California  
Los Angeles, CA 90007-0742  
jvidale@usc.edu*

Christopher J. Vogl

*Center for Applied Scientific Computing  
Lawrence Livermore National Laboratory  
Livermore, CA 94550  
chris.j.vogl@gmail.com*

William S. D. Wilcock

*School of Oceanography  
University of Washington  
Seattle, WA 98195-7940  
wilcock@uw.edu*

**Abstract**—Real-time tsunami warning in the nearfield is considerably more difficult than producing warnings for distant events. Although in some cases strong shaking will provide the only warning, there are several situations in which better early tsunami warning systems could be critical. We discuss some of the issues that arise, particularly the difficulty of interpreting ocean bottom pressure recordings in the near source region, and make some recommendations for future research and first steps toward a better warning system for the Pacific Northwest.

**Index Terms**—tsunami, earthquake, subduction zone, early warning

## I. INTRODUCTION

The Early Warning Offshore Cascadia project<sup>1</sup>, funded in part by the Gordon & Betty Moore Foundation, has been investigating the potential costs and benefits of expanding offshore data collection capabilities in relation to the improvement of early warning capabilities for both seismic and tsunami

This work was performed, in part, under the auspices of the U.S. Department of Energy by Lawrence Livermore National Laboratory under Contract DE-AC52-07NA27344 and supported, in part, by the Gordon & Betty Moore Foundation, and NSF Hazard SEES grant EAR-1331412 (the M9 Project). LLNL-CONF-756571

<sup>1</sup><http://cascadiaoffshore.org/>

components of a subduction zone megathrust earthquake or other offshore events. The benefits of better scientific understanding of the Cascadia Subduction Zone are also taken into consideration. An overview was given at the Oceans '16 meeting [63] and a white paper summarizing many findings and recommendations is currently in preparation, based in part on discussions at a workshop held in April, 2017 [55]. This paper contains a brief summary of some of the issues related to the development of better tsunami early warning systems for offshore Cascadia events.

## II. THE NEED FOR TSUNAMI EARLY WARNING

Tsunami warnings for the Pacific Northwest are issued by the National Tsunami Warning Center (NTWC) in Palmer, AK, operated by NOAA. These warnings are currently based on a combination of seismic information used to estimate the location and magnitude of the earthquake, and ocean bottom pressure (OBP) data collected at a sparse set of locations in the deep ocean that are transmitted to the warning centers by DART buoys (Deep-ocean Assessment and Reporting of Tsunamis, [50], [58]). The OBP data at sites distant from the tsunami source reveal changes in the hydrostatic pressure

due to the increased surface elevation as a long-wavelength tsunami passes by. These data are used in real time to perform source inversion and to estimate the tsunami accurately enough that more distant coastal regions can be adequately warned. This system works well for providing tsunami warnings in the Pacific Northwest for far-field tsunamis, such as those originating in Japan, Alaska, or Chile for example.

However, this warning system will be of limited use for tsunamis originating in the nearfield, in particular from thrust earthquakes on the Cascadia Subduction Zone (CSZ) that runs from northern California to Vancouver Island. This region is known to have experienced an Mw 9 size earthquake on January 26, 1700, and geologic evidence (including tsunami deposits and turbidites) suggests that around 20 ~ Mw 9 earthquakes and numerous Mw 8–8.5 earthquakes have occurred over the past 10,000 years [6], [19], [36]. The tsunami from such an earthquake will reach many coastal locations in less than 30 minutes, roughly the same time it could take to reach the closest DART buoys. Moreover, whereas the OBP data at sparse DART locations is often adequate for a distant source, a tsunami generated from a nearfield source is sensitive to the spatial and temporal distribution of seafloor motion. A much denser network of sensors on the seafloor in the nearfield region would provide greatly enhanced prediction abilities.

The inadequacy of tsunami warning that relies on DART buoys can be observed in a simulated CSZ event. Figure 1(a) shows a hypothetical slip distribution and corresponding rupture onset on the CSZ sampled from a distribution of random earthquakes with a specified correlation length, taken from a set of 1300 such earthquakes presented in [48]. A time-dependent kinematic slip has been assigned, initiating at about 45°N and rupturing bilaterally over approximately 280 seconds as indicated in 1(b). Figure 2 shows the sea surface displacement as the tsunami forms and propagates, along with the location of the three DART buoys in the vicinity. Note that it takes about 20 minutes for the waves to first reach the nearest DART location and that waves are striking the coast within this time frame. This is because the wave speed is  $\sqrt{gh}$  (where  $h$  is the water depth and  $g$  the acceleration due to gravity), which results in the waves heading offshore moving much faster than the waves approaching shore. This wave speed also causes the shore-bound waves to be compressed and amplified due to shoaling as they pass onto the shallow continental shelf. Also note that one hour after the earthquake starts, the first wave is still passing through the Strait of Juan de Fuca and edge waves are visible elsewhere on the coast.

Granted, the strong shaking along the coast will be the only warning that most people will receive for a major earthquake, and advance planning and education will be essential to insure that people know to move as quickly as possible to high ground, as far from sea level as possible. However, there are several reasons why it is also desirable to develop more effective methods for providing nearfield tsunami warnings. These include:

- Although the first wave will arrive at coastal locations near the earthquake source region very quickly, the

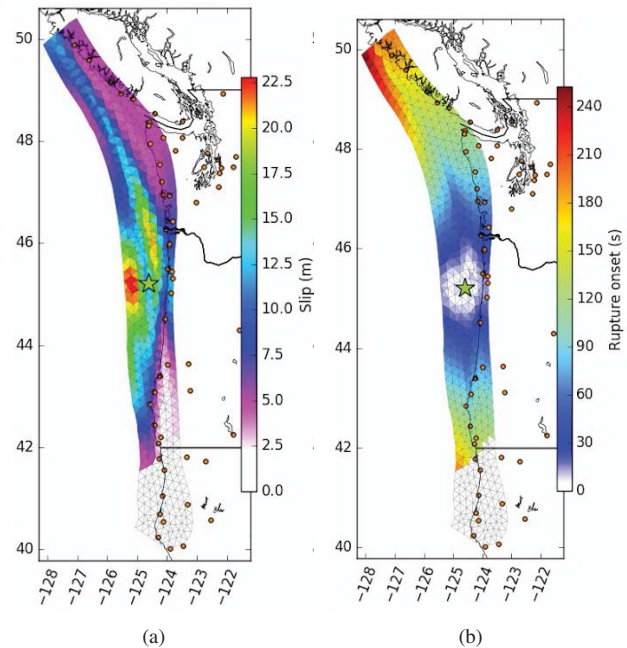


Fig. 1. Hypothetical CSZ earthquake, realization #1297 from [48]. (a) shows the slip distribution on the triangulated fault surface. (b) shows the rupture time, with the star showing the epicenter.

tsunami hazard often goes on for many hours after the first wave has arrived because of edge waves propagating along the continental shelf, which can combine with reflections or resonances due to coastal features. It is particularly important for first responders to be able to enter the inundation zone as soon as it is safe to do so, but no sooner.

- A CSZ earthquake may not rupture the full length of the subduction zone. The tsunami arising from an earthquake on the southern edge of the CSZ, for example, could take more than an hour to reach the coast of Washington State or British Columbia and would provide less warning in the form of local shaking.
- Coastal regions in the Salish Sea, such as Seattle, WA or Vancouver, BC, still face tsunami hazard, but the first wave will not arrive until more than two hours after the earthquake due to the relatively slow propagation through the Strait of Juan de Fuca, as seen in Figure 2. As in the previous two situations, more detailed tsunami predictions over the time scale of many hours could be valuable.
- There is increasing interest in providing maritime tsunami warnings in addition to inundation warnings. Many coastal regions, particularly in the Salish Sea, will experience very dangerous currents for an extended periods of time even if there is little flooding nearby.
- Some earthquakes generate much bigger tsunamis than might be expected from the ground shaking they produce. These so-called “tsunami earthquakes” have been deadly in the nearfield even in cases when the earthquake was

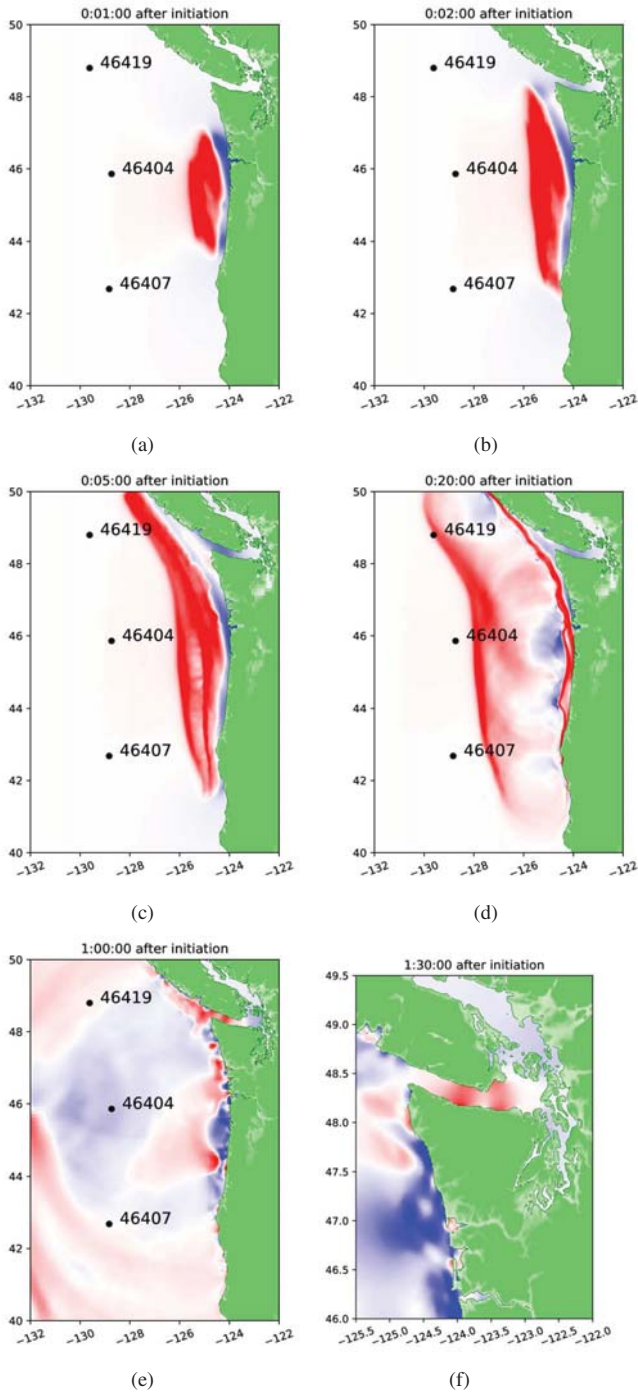


Fig. 2. Six frames from a tsunami simulation using the kinematic earthquake rupture shown in Figure 1. (a-c) show the developing tsunami at 1, 2, and 5 minutes after initiation. (d-e) show the waves at 20 minutes and 1 hour. (f) shows a zoomed view around Washington State and southern B.C. at 1.5 hours. The numbered points indicate DART buoy locations. Red and blue colors saturate at  $\pm 2\text{m}$  surface elevation relative to sea level.

not felt [17], [29], as in the case of the 1992 Nicaragua earthquake [30].

- Tsunamis are sometimes caused by submarine mass failures on the continental slope that result from relatively weak earthquakes or are aseismic [7], [44]. As in the previous example, better nearfield tsunami warning systems could provide the only warning for nearby coastal regions.

An improved warning system could provide more detailed information about the wave heights, expected arrival times, and later arriving waves than is available from the current warning system, as well as providing critical warnings for events not connected to strong shaking. In addition to more timely warnings to the public, such a system could greatly aid first responders and provide better situational awareness to emergency managers.

### III. APPROACHES TO IMPROVING TSUNAMI EARLY WARNING

For nearfield warnings, the US system currently relies primarily on rapid point source seismic inversion that estimates the most basic earthquake parameters such as location, magnitude, and faulting style. The median response time for availability of such information is  $\sim 8$  minutes [54]; however, this information is of limited immediate use because it is not accompanied by a forecast of the expected tsunami wave heights. Additionally, the current system relies mostly on regional seismic data and is prone to a well known condition (magnitude saturation) where the system cannot distinguish between large and very-large earthquakes. Thus, even if a tsunami forecast were to be made for a major earthquake, it would likely severely underestimate wave heights. This was the case during the 2011 M9 Tohoku-oki earthquake: the initial warning was far too low and was not updated until 13 hours after the onset of the earthquake [28].

To address this, a project is now underway to incorporate geodetic observations at onshore GNSS stations into the rapid source inversion process. Geodesy circumvents the magnitude saturation problem [47] and produces reliable estimates of earthquake source characteristics in the first 1–2 minutes. As demonstrated in [46], this in turn leads to significantly improved rapid predictions for some recent historical events. This is now being tested for the 1300 random CSZ earthquake realizations developed in [48] by comparing full simulations starting with the correct hypothetical source (the presumed true tsunami) with simulations based on approximate sources obtained from rapid source inversion using synthetic seismograms and GNSS observations generated by applying a seismic modeling code [14] to the original source. Incorporation of this technology into the warning centers could lead to immediate improvements in nearfield tsunami amplitude forecasting. As part of this modeling project, a collection of hypothetical offshore gauges are also being introduced so that time series of sea surface elevation at each of these locations will be available for each of the 1300 realizations. This will provide a valuable database for exploring the possibility of making

additional improvements in the forecasting if this additional data were available. This data will be collected on a dense network of synthetic offshore gauges, which will also allow experimenting with using different subsets of the data in order to explore the density of gauges that are required to obtain significantly improved forecasts.

This synthetic data will consist of sea surface and velocity “observations”, which are easily available in the simulations but not easily acquired in the real world, at least not in the vicinity of the earthquake source. At distant DART buoys the hydrostatic pressure measured by BPRs gives a good estimate of the surface elevation as a long-wavelength tsunami passes by, but in the source region the pressure variations due to seafloor acceleration and hydroacoustic waves generated by the earthquake in the compressible sea water make it much more difficult to determine sea surface motion from bottom pressure. This is further explored in Section IV.

It is important here to distinguish between *direct* and *indirect* approaches to warning. In indirect warning one must first characterize the earthquake and then use that, and some assumptions, to infer the tsunami initial condition and run a model to propagate it to shore. There is no measurement of the hazardous phenomenon itself. Direct warning in turn involves inference about the expected coastal hazard directly from a measurement of the tsunami farther from shore.

There are a number of possible ways to directly measure the tsunami as it approaches the shore. For example, it is possible to use high-frequency (HF) radar to estimate currents based on Bragg scattering, with the possibility of detecting tsunamis up to 200 km offshore (see e.g., [22], [41], [42]). This has been deployed by Ocean Networks Canada at Tofino, British Columbia, since 2015 [20], [21].

Moored GNSS buoys would be another approach to direct measurement of the sea surface. These buoys measure vertical position and as such are directly sensitive to the sea-surface disturbance. A small network of such buoys was operational during the 2011 M9 Tohoku-oki earthquake [25] and recorded open ocean amplitudes as large as  $\sim 7$  m. When the Japanese buoy network was conceived they were constrained to being deployed no further than  $\sim 30$  km from shore due to the requirement of an onshore reference GNSS station. However, with advancements in GNSS positioning techniques this is no longer necessary and the buoys could be deployed anywhere in the open ocean and be able to reliably detect vertical signals larger than 5-10 cm [18].

Another, more popular approach to direct warning is to use real-time cabled pressure recordings from the seafloor. As we will see in the next section this is a non-trivial issue. However the approach remains popular; Japan is leading the way with the S-net network [32], which consists of more than 800 km of fiber optic cable covering the Japan trench with 150 nodes, spaced roughly every 30 km. Each node contains absolute pressure, strong motion, broadband, and short period sensors. Although smaller in scope, similar real-time cables exist at the Cascadia subduction zone on both the Canadian and U.S. portions of the system [8], [15], [26], [56].

Finally, tsunami warning efforts do not happen in isolation. In the U.S., the ShakeAlert earthquake early warning system [34] should be operational by the end of 2018. To begin with, the system will rely on on-shore seismic and geodetic measurements to provide rapid estimates of the earthquake source and its associated shaking. As it develops it will likely ingest offshore seismic measurements and potentially high-rate geodetic measurements such as seafloor strain or vertical deformation from pressure data. Because these data products will be developed, tested, and deployed for a similar mission they should be considered for use in an indirect tsunami warning approach as well.

#### IV. OCEAN BOTTOM PRESSURE NEAR THE SOURCE

The DART network is a critical component of the farfield warning system since changes in OBP accurately reflect the amplitude of a long wavelength tsunami passing by. It is not straightforward, however, to use OBP to determine the tsunami amplitude in the immediate source region. Several problems arise.

If water were incompressible, then a rapid seafloor uplift over a broad area would be matched by a corresponding uplift in the sea surface, and no change in the water depth. So even if it were possible to measure the hydrostatic pressure alone at the sea floor, this would not change over the short time scale of the earthquake. It is only after the sea surface disturbance starts to propagate away as gravity waves that the water depth will change. Moreover, the compressibility of water must be taken into account since the seismic waves in the earth are transmitted as hydroacoustic waves in the water column. In fact the surface does not begin to move until the first acoustic wave reaches the surface and the motion of the surface is mediated by these waves bouncing between the seafloor and the surface. For rapid seafloor accelerations, pressure variations due to the hydroacoustic waves can be orders of magnitude larger than the changes in hydrostatic pressure due to depth variations. This is exhibited, for example, in the OBP observations at two BPRs in the source region of the 2003 Tokachi-Oki event [10], [40], [52] and at the same pressure gauges for the more distant 2011 Tohoku event [45].

The dominant acoustic frequency observed in the source region is  $f_1 = c_s/4H$  where  $c_s \approx 1500$  m/s is the speed of sound in water and  $H$  is the depth. In a depth of 4500 m, for example, this is  $f_1 \approx 0.125$  Hz, with a corresponding period of 12 seconds, which is 4 times the one-way travel time of acoustic waves from the sea floor to the surface. Porous sedimentary layers often increase the effective depth, decreasing the dominant frequency (e.g. [2], [40]).

If the vertical velocity of the seafloor is  $v(t)$ , then changes in pressure at the seafloor due to the acceleration  $\dot{v}(t)$  are approximated by  $p'(t) = \rho c_s \dot{v}(t)$ , where  $\rho \approx 1025$  kg/m<sup>3</sup> is the density of sea water [38]. The acoustic pressure rises only until the first reflected waves from the surface arrive at the seafloor and so the amplitude of the acoustic waves generated depends on the relation between the rise time of the seafloor, the travel time and the peak acceleration.

If the seafloor were moving with constant acceleration then the acoustic waves would oscillate about an average pressure corresponding to the force required to maintain this acceleration of the water column, which has mass  $\rho H$  per unit seafloor area. This gives a pressure of  $\rho H \dot{v}(t)$ , which must be added to the hydrostatic pressure  $\rho g H$  (which can be viewed as the force required to resist gravitational acceleration).

Since a BPR records all of these pressures, we can expect a complicated signal in the source region. To clarify this, in Figures 3 and 4 we present sample results from on-going work in which we are attempting to better understand these effects by developing a fully coupled numerical model of seismic, acoustic, and gravity waves [37], [61]. Other good discussions and simulations of similar problems can be found in the literature, e.g. [1], [12], [13], [27], [35], [38], [51], [53].

The simple example presented here is from a acoustics plus gravity simulation of a two-dimensional vertical slice of the ocean, with a flat bottom at depth  $H = 4500$  m and a horizontal extent of more than 300 km. A gaussian uplift of the seafloor is introduced via a boundary condition in the linear acoustics equations, rising to  $A = 10$  m elevation at the center of the domain ( $x = 0$ ). The final deformation is  $Z(x) = A \exp(-(x/25)^2)$  where  $x$  is measured in km here. The rise is a smooth half-period cosine function over a rise time  $T_r = 50$  seconds, giving a seafloor acceleration of

$$\dot{v}(x, t) = \frac{1}{2} (\pi/T_r)^2 \cos(\pi t/T_r) Z(x) \quad \text{for } t \leq T_r. \quad (1)$$

Figure 3 shows the seafloor deformation and the resulting surface deformation at five selected times. With this rise time, the surface tracks the seafloor motion fairly well over the first 40 seconds but over longer time scales the inclusion of gravity leads to the formation of two outward propagating tsunami waves, propagating at speeds  $\pm c_g$  where the gravity wave speed is  $c_g = \sqrt{gH} \approx 210$  m/s.

In order to compare pressures with surface elevation in the plots, it is convenient to represent the pressure in units of “meters of sea water” by dividing pressures by  $\rho g$ . Figure 4 shows the seafloor pressure in these units recorded at two synthetic gauges at  $x = 0$ , the center of the uplift, and at  $x = 75$  km, outside the region of uplift. The latter gauge, shown in Figure 4(a), clearly shows that the bottom pressure (black curve) includes a strong acoustic wave with a period of 12 seconds. This wave is generated in the source region and spreads laterally while predominantly propagating in the vertical direction. Filtering out this acoustic wave by computing a running 12-second average of the pressure gives the red curve, which accurately tracks the change in hydrostatic pressure expected from the propagating tsunami (which in our units should agree with the surface elevation, shown by the blue curve).

The pressure gauge at  $x = 0$ , shown in Figure 4(b) over a shorter time period, shows a more complex structure. The seafloor rise is shown in green and the surface elevation shown in blue tracks this fairly well until the gravity waves start to propagate away and then the surface drops back down

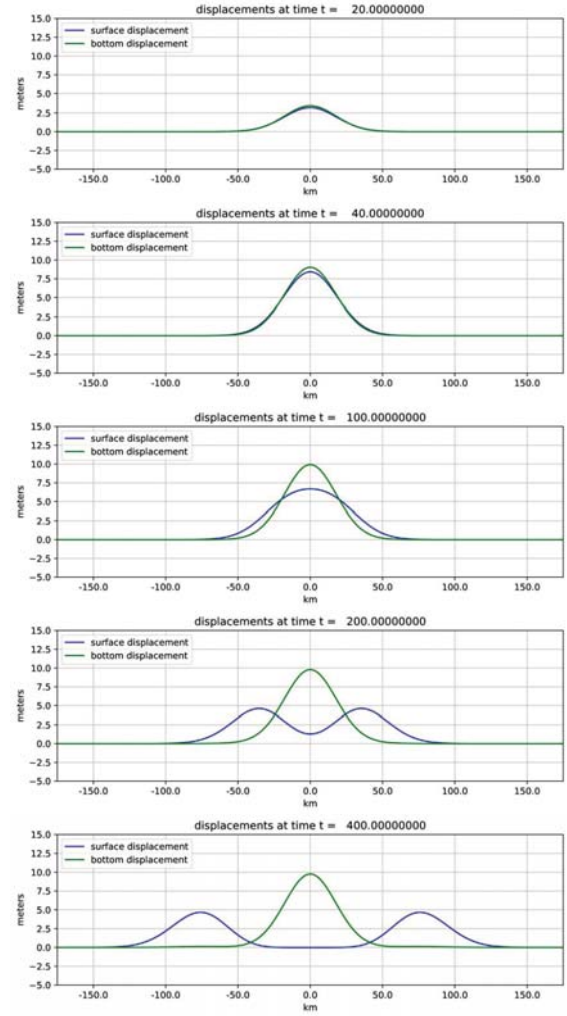
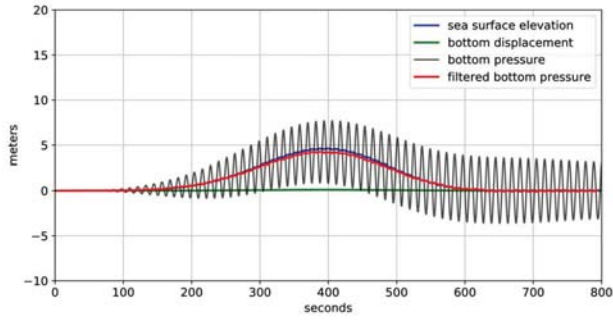


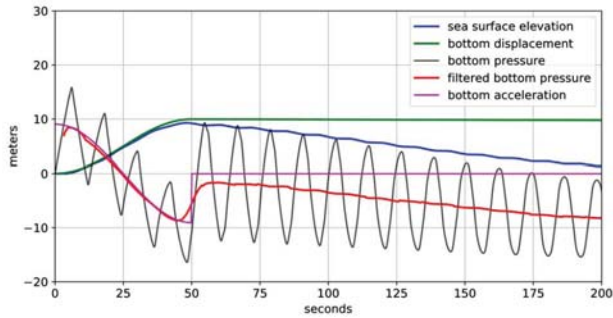
Fig. 3. Seafloor and surface displacements at 5 times, as computed using acoustics plus gravity in a 4500 m deep ocean. The seafloor deformation is a Gaussian hump rising over 50 seconds. The inclusion of gravity leads to the formation of gravity waves, the tsunamis that propagate away in both directions at later times.

toward 0. The pressure shown in black exhibits the acoustic oscillation, and filtering this out as before gives the red curve. During the 50 second rise time this closely tracks the sum of the pressure due to bottom acceleration (given by  $(H/g)\dot{v}$  in our units), which is shown as the magenta curve, together with the change in hydrostatic pressure expected from the varying ocean depth (which can be obtained by subtracting the bottom displacement from the surface displacement).

If this experiment is repeated with a longer rise time  $T_r$ , then the amplitude of the bottom acceleration  $\dot{v}$  decreases like  $1/T_r^2$ , according to (1), and the amplitude of the acoustic waves generated decreases accordingly. In this case the bottom pressure more closely matches the hydrostatic pressure alone. (The seismic waves generated by a slower slip also have smaller amplitude, which is consistent with the fact that slow slipping “tsunami earthquakes” generate a larger tsunami than



(a) At 75 km, away from the uplift



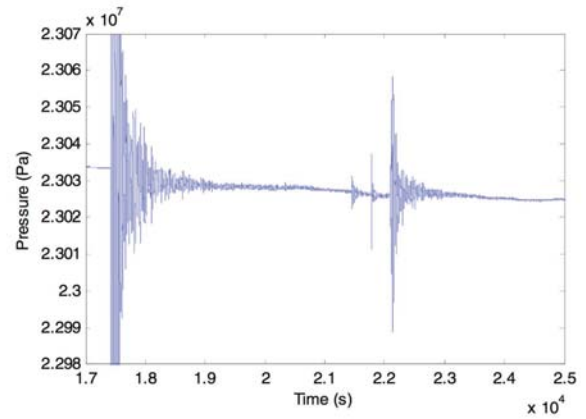
(b) At  $x = 0$  km, the center of the uplift

Fig. 4. Pressure gauge and displacement time series for the simulation shown in Figure 3, with a Gaussian hump seafloor displacement rising over 50 seconds. Pressures are in units of meters of sea water. See the text for discussion.

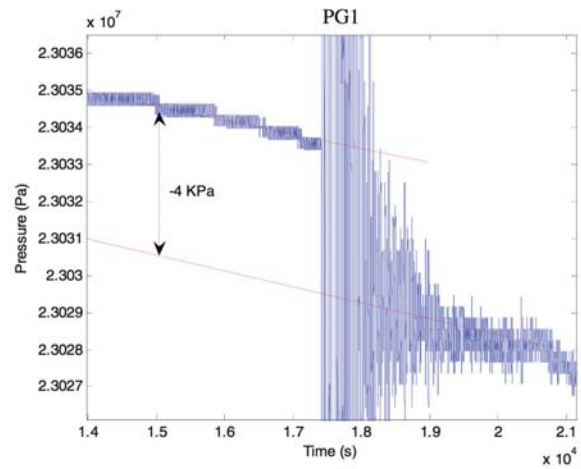
expected from the ground motion.)

On the other hand, larger accelerations will give rise to acoustic waves that are orders of magnitude larger, even if the seafloor displacement is much smaller. The peak seafloor acceleration in the test shown here is only  $0.0197 \text{ m/s}^2 \approx 0.002g$ .

Figure 5 shows raw pressure data observed at the JAMSTEC BPR denoted PG1, which was deployed off the coast of Hokkaido at  $(41.70^\circ\text{N}, 144.44^\circ\text{E})$ , within the source region of the 2003 Mw 8.1 Tokachi-Oki event. The initial mean water depth was 2283 m at this location, giving a hydrostatic pressure of roughly  $2.3 \times 10^7$  Pa. The residual seafloor displacement at this location was roughly +0.4 m, which agrees with the offset of  $-4$  kPa in hydrostatic pressure shown in Figure 5(b) due to the shallower depth after the earthquake. The relatively slow change in depth as the tsunami propagates away from the source region is completely masked by the large amplitude acoustic waves, with pressure amplitude greater than 40 KPa ( $\sim 4$  m sea water), 10 times larger than the seafloor displacement. Analysis of the acoustic waves (see e.g., [10], [39], [40], [52]) shows that the dominant frequency is somewhat lower than the fundamental frequency  $f_1$  due to the sediments in this region. Of course the complex seafloor motion during an earthquake contains a range of frequencies. Much of the energy of the earthquake propagates away as pure acoustic waves at frequencies higher than the fundamental frequency  $f_1$ . Frequencies lower than  $f_1$  can not be supported



(a) Over 8000 seconds showing main shock and three aftershocks.



(b) Over 7000 seconds with expanded pressure scale.

Fig. 5. Raw pressure data sampled at 10 Hz, observed at JAMSTEC pressure gauge PG1 during the 2003 Tokachi-Oki Earthquake. Figures from Li [39], with permission. See the text for more discussion.

as acoustic waves in the ocean and instead lead to “forced oscillations” that feed into the generation of the tsunami, at least down to the gravity wave frequency  $f_g \sim \sqrt{g/H}$ , below which energy propagates away as gravity waves faster than surface displacement can accumulate. See, e.g. [38] for more discussion.

## V. NECESSARY RESEARCH AND ALGORITHM DEVELOPMENT

The example just shown illustrates that OBP recordings in the nearsource region contain a mixture of hydrostatic, hydroacoustic, and direct seafloor acceleration forces, and can be difficult to interpret even in the simplest case. In order to accurately estimate the tsunami that is being generated within the first few minutes, it is necessary to better understand the pressure signals that will be generated from a complex rupture event, through a combination of numerical simulations and interpretation of available BPR records in nearsource locations.

Several references cited above address these issues, but much more work is needed.

One interesting question is whether OBS data could be used together with BPR data to better constrain the actual seafloor motion. It is very difficult to obtain accurate ground displacements by integrating recorded accelerations. Small baseline changes associated with rotations and tilts, when doubly integrated, lead to large spurious apparent displacement artifacts. [59]. The conventional method of attempting to correct for these effects include high-pass filtering, which removes the signal of interest, and/or applying baseline corrections [11] which is non-unique and not achievable in realtime. Onshore, the combination of inertial and non-inertial estimates of ground motion from collocated seismic and GNSS sensors leads to accurate retrieval of displacements across a broad frequency range [9]. It needs to be investigated if pressure data, as a non-inertial proxy for vertical motion, could serve the same purpose offshore. Another possible approach to obtaining ground displacement is to incorporate sensors that obtain 6-component accelerometer data to simultaneously observe both rotational and linear motions [49].

Several recent papers (e.g. [23], [43], [57]) have explored the use of data assimilation to incorporate real-time observations of sea surface elevation into a running tsunami model in order to dynamically improve the estimate of the waves approaching shore. This work has mostly been based on synthetic data generated from a tsunami model, from which it is possible to derive the sea surface elevation directly. As we have seen, it is non-trivial to determine the sea surface elevation from OBP observations, particularly during the earthquake in the source region but also due to strong acoustic waves for some time afterward. Similarly, source inversion from DART data in the farfield assumes that surface elevation can be directly inferred from OBP. To make effective use of such techniques in the nearfield will require better approaches to determining the sea surface elevation dynamically in the nearfield.

Another open question is the required density and optimal placement of sensors. Due to the high cost of an offshore network, it is desirable to minimize the number of sensors required. There are also open questions regarding whether it is better to place sensors near shore on the continental shelf (which might be best for directly measuring the approaching waves and later edge wave activity) or in deeper water beyond the shelf that waves would reach more quickly due to the increase in gravity wave speed with depth. Numerous other considerations come into placement; for example the fact that hydroacoustic waves generated near the source have fundamental frequencies  $f_1$  that depend on the depth at the source location. While these strong pressure oscillations can propagate long horizontal distances into deeper water, they do not propagate into water that is shallower than the depth of the source location. This suggests that much less acoustic noise would be present in OBP measurements in shallow water. See [3] for a clear illustration of this in simulations of the 2012 Haida Gwaii earthquake. Practical concerns also come into placement, e.g., the relative expense of deploying and

maintaining instruments, and susceptibility to damage from submarine mass failures on the continental slope or from fishing trawlers.

## VI. RECOMMENDATIONS

The development of more effective nearfield tsunami warnings for the Cascadia Subduction Zone will require additional research on the issues outlined above. In particular, we believe that a better understanding of OBP observations and their use in estimating details of the tsunami as it develops in real time is a critical component.

For a practical warning system, a hierarchy of models will likely be required for different time scales. For example, the best strategy may involve using seismic/GNSS data in the first minute, supplemented by bottom pressure and sea surface elevation data on time scales of 5-10 minutes and then tide gauge or water current data at later times. Data assimilation to incorporate data into evolving tsunami models is potentially a powerful tool, particularly if it can be coupled with the use of seismic and hydroacoustic observations, and not require direct observation of the surface elevation.

As a first step toward an offshore network in the Pacific Northwest, we suggest that the NSF Ocean Observatories Cabled Array, which crosses the Cascadia subduction zone off central Oregon, and the Ocean Networks Canada NEPTUNE cabled observatory, off Vancouver Island, should be used to test instrumentation and the implementation of a prototype tsunami warning system that could then be expanded to cover the full subduction zone. We are studying synthetic data to quantify the potential benefits of incorporating such a network into tsunami forecasting models, and to better understand how this might compare with alternative sensor platforms that do not require a seafloor cable.

Computational algorithms and software must be adequately validated to give confidence in the forecasts. Simulations based on synthetic data are part of this, but the use of real observations from locations where sensors were in place during seismic events is also critical. The 2003 Tokachi-Oki event is one of the few sources of such data for a significant earthquake [10], [40], [52], but sensors now in place on the cabled observatories offshore Japan [31], [33] and Cascadia [8], [56] and those being increasingly deployed as part of temporary networks of autonomous instruments for geodetic [62] and seismic [60] experiments could provide additional data in the future.

We also recommend serious consideration of a sensor system for the Salish Sea based on observations near the entrance of the Strait of Juan de Fuca (which might take the form of BPRs, HF radar, GNSS buoys, and/or other technologies). Tsunami simulations from hypothetical events show that most significant populations centers in the Salish Sea are not impacted by a wave until several hours after it first enters the Strait. Preliminary results from on-going work also show that observations in the Strait alone can be used to produce very accurate estimates of the tsunami impact in this enclosed body of water.

The design of an early warning system should take into account the needs and desires of the warning centers and emergency management communities. Recent findings from the 2017 Mexico earthquakes suggest that for that for Earthquake Early Warning (EEW), too much information can overwhelm and slow down the response [5]. The local tsunami warning problem is fundamentally different from EEW in that the desired action is for the public to evacuate as quickly as possible along pre-determined routes and to pre-determined locations. One possibility might be to produce several different scenario maps for each community with different severity levels. Each community could then plan its response for the different warning or severity levels. Once the tsunami has been characterized by the system, it can rapidly identify which severity level applies to communities in different coastal regions. A similar approach is being taken in California for Maritime hazards [64]. Rapid identification of severity has been explored in [24], for example, in the context of rapid estimation of inundation by matching to a set of pre-computed scenarios, and in [4] in the context of clustering random earthquake realizations based on tsunami characteristics for probabilistic hazard assessment.

More input from emergency managers and first responders is required to help design a warning system that is both feasible and useful. This work should also be integrated with efforts to improve the resilience of coastal infrastructure, and to locate and design appropriate vertical evacuation structures in coastal regions where it may be impossible to reach sufficiently high ground in the available time following a nearfield event (e.g., [16]).

## VII. CONCLUSIONS

Developing better tsunami warning systems for nearfield events is challenging but important, since the existing DART buoy systems offshore Oregon and Washington is not designed to provide an adequate tsunami warning for a nearfield megathrust earthquake or slope failure. There is a need to provide near-real-time estimates of the wave height and arrival time for primary and secondary arrivals, particularly if coastal residents are not adequately informed of the immediate risk by strong ground shaking. There are several technical and scientific challenges in implementing a fully functional tsunami warning system, such as how best to instrument the seafloor with real-time telemetry, and how best to identify seafloor and sea surface deformation from data acquired during the earthquake. Modeling studies also need to be undertaken to optimize the spacing and distribution of sensors and to develop techniques to update running tsunami models with real time data.

In Cascadia there is an opportunity to accelerate efforts to address these solvable problems, by taking advantage of existing cabled seafloor observatories to test approaches to data acquisition and to the incorporation of refined modeling techniques into prototype early warning systems. At the same time, it will be critical to work with coastal communities, disaster managers, and federal and state agencies to ensure that the design of a subduction zone wide warning system is part of

ongoing efforts to improve coastal resilience and preparedness, so that the warning leads to an effective response that saves lives and minimizes disruption. Although we are now at a stage to fully conceive of an operational system, future research and development is required before a system can be fully realized.

## DISCLAIMER

This document was prepared, in part, as an account of work sponsored by an agency of the United States government. Neither the United States government nor Lawrence Livermore National Security, LLC, nor any of their employees makes any warranty, expressed or implied, or assumes any legal liability or responsibility for the accuracy, completeness, or usefulness of any information, apparatus, product, or process disclosed, or represents that its use would not infringe privately owned rights. Reference herein to any specific commercial product, process, or service by trade name, trademark, manufacturer, or otherwise does not necessarily constitute or imply its endorsement, recommendation, or favoring by the United States government or Lawrence Livermore National Security, LLC. The views and opinions of authors expressed herein do not necessarily state or reflect those of the United States government or Lawrence Livermore National Security, LLC, and shall not be used for advertising or product endorsement purposes.

## REFERENCES

- [1] A. Abdolali, C. Cecioni, G. Bellotti, and P. Sammarco, "A depth-integrated equation for large scale modeling of tsunami in weakly compressible fluid," *Coastal Engineering Proceedings*, vol. 1, no. 34, p. 9, 2014.
- [2] A. Abdolali, J. T. Kirby, and G. Bellotti, "Depth-integrated equation for hydro-acoustic waves with bottom damping," *Journal of Fluid Mechanics*, vol. 766, 2015.
- [3] Abdolali Ali, Cecioni Claudia, Bellotti Giorgio, and Kirby James T., "Hydro-acoustic and tsunami waves generated by the 2012 Haida Gwaii earthquake: Modeling and in situ measurements," *Journal of Geophysical Research: Oceans*, vol. 120, no. 2, pp. 958–971, 2015.
- [4] L. M. Adams, R. J. LeVeque, D. Rim, and F. I. Gonzalez, "Probabilistic source selection for the Cascadia Subduction Zone. Results from a study supported by FEMA Region IX," 2017. [Online]. Available: <http://depts.washington.edu/ptha/FEMA>
- [5] R. Allen, E. Cochran, T. Huggins, S. Miles, and D. Otegui, "Lessons from Mexico's earthquake early warning system," EOS (in press), 2018.
- [6] B. F. Atwater, S. Musumi-Rokkaku, K. Satake, Y. Tsuji, K. Ueda, and D. K. Yamaguchi, *The Orphan Tsunami of 1700: Japanese Clues to a Parent Earthquake in North America*, 2nd ed. University of Washington Press, 2015, u.S. Geological Survey Professional Paper 1707.
- [7] J. P. Bardet, C. E. Synolakis, H. L. Davies, F. Imamura, and E. A. Okal, "Landslide tsunamis: Recent findings and research directions," *Pure and Applied Geophysics*, vol. 160, no. 10, pp. 1793–1809, 2003.
- [8] C. R. Barnes, M. M. R. Best, F. R. Johnson, and B. Pirenne, "NEPTUNE Canada: Installation and initial operation of the world's first regional cabled ocean observatory," in *Seafloor Observatories*, ser. Springer Praxis Books. Springer, Berlin, Heidelberg, 2015, pp. 415–438.
- [9] Y. Bock, D. Melgar, and B. W. Crowell, "Real-time strong-motion broadband displacements from collocated GPS and accelerometers," *Bulletin of the Seismological Society of America*, vol. 101, no. 6, pp. 2904–2925, 2011.
- [10] A. Bolshakova, S. Inoue, S. Kolesov, H. Matsumoto, M. Nosov, and T. Ohmachi, "Hydroacoustic effects in the 2003 Tokachi-oki tsunami source," *Russian Journal of Earth Sciences*, vol. 12, no. 2, 2011. [Online]. Available: <https://cyberleninka.ru/article/n/hydroacoustic-effects-in-the-2003-tokachi-oki-tsunami-source>

- [11] D. M. Boore and J. J. Bommer, "Processing of strong-motion accelerograms: needs, options and consequences," *Soil Dynamics and Earthquake Engineering*, vol. 25, no. 2, pp. 93–115, 2005.
- [12] C. Cecioni and G. Bellotti, "On the resonant behavior of a weakly compressible water layer during tsunamigenic earthquakes," *Pure and Applied Geophysics*, vol. 175, no. 4, pp. 1355–1361, 2018.
- [13] Chierici Francesco, Pignagnoli Luca, and Embriaco Davide, "Modeling of the hydroacoustic signal and tsunami wave generated by seafloor motion including a porous seabed," *Journal of Geophysical Research: Oceans*, vol. 115, no. C3, 2010.
- [14] B. W. Crowell, D. A. Schmidt, P. Bodin, J. E. Vidale, J. Gombert, J. Renate Hartog, V. C. Kress, T. I. Melbourne, M. Santillan, S. E. Minson *et al.*, "Demonstration of the Cascadia G-FAST geodetic earthquake early warning system for the Nisqually, Washington, earthquake," *Seismological Research Letters*, vol. 87, no. 4, pp. 930–943, 2016.
- [15] J. R. Delaney and D. S. Kelley, "Next-generation science in the ocean basins: Expanding the oceanographer's toolbox utilizing submarine electro-optical sensor networks," in *Seafloor Observatories*, ser. Springer Praxis Books. Springer, Berlin, Heidelberg, 2015, pp. 465–502.
- [16] R. Freitag *et al.*, "Project Safe Haven: Pacific County Tsunami Vertical Evacuation on the Washington Coast," Washington State Emergency Management Division, Tech. Rep., 2011. [Online]. Available: [https://mil.wa.gov/uploads/pdf/emergency-management/haz\\_safehavenreport\\_pacific.pdf](https://mil.wa.gov/uploads/pdf/emergency-management/haz_safehavenreport_pacific.pdf)
- [17] E. L. Geist, "Complex earthquake rupture and local tsunami," *Journal of Geophysical Research*, vol. 107, no. B5, p. 2086, 2002.
- [18] J. Geng, Y. Bock, D. Melgar, B. W. Crowell, and J. S. Haase, "A new seismogeodetic approach applied to GPS and accelerometer observations of the 2012 Brawley seismic swarm: Implications for earthquake early warning," *Geochemistry, Geophysics, Geosystems*, vol. 14, no. 7, pp. 2124–2142, 2013.
- [19] C. Goldfinger, C. H. Nelson, A. E. Morey, J. R. Patton, E. Karabanov, J. Gutierrez-Pastor, and A. T. Eriksson, *Turbidite Event History—Methods and Implications for Holocene Paleoseismicity of the Cascadia Subduction Zone*. U.S. Geological Survey Professional Paper 1661-F, 2012. [Online]. Available: [https://pubs.usgs.gov/pp/pp1661f/pp1661f\\_text.pdf](https://pubs.usgs.gov/pp/pp1661f/pp1661f_text.pdf)
- [20] S. T. Grilli, M. Shelby, A. Grilli, C.-A. Guérin, S. Grosdidier, and T. Insua, "Algorithms for tsunami detection by high frequency radar : Development and case studies for tsunami impact in British Columbia, Canada," in *The 26th International Ocean and Polar Engineering Conference*. International Society of Offshore and Polar Engineers, 2016. [Online]. Available: <https://www.onepetro.org/conference-paper/ISOPE-I-16-566>
- [21] C.-A. Guérin, S. T. Grilli, P. Moran, A. Grilli, and T. Insua, "Tsunami detection by high frequency radar using a time-correlation algorithm: Performance analysis based on data from a HF radar in British Columbia," in *The 27th International Ocean and Polar Engineering Conference*. International Society of Offshore and Polar Engineers, 2017. [Online]. Available: <https://www.onepetro.org/conference-paper/ISOPE-I-17-506>
- [22] K.-W. Gurgel, A. Dzvonkovskaya, T. Pohlmann, T. Schlick, and E. Gill, "Simulation and detection of tsunami signatures in ocean surface currents measured by HF radar," *Ocean Dynamics*, vol. 61, no. 10, pp. 1495–1507, 2011.
- [23] A. R. Gusman, A. F. Sheehan, K. Satake, M. Heidarzadeh, I. E. Mulia, and T. Maeda, "Tsunami data assimilation of Cascadia seafloor pressure gauge records from the 2012 Haida Gwaii earthquake," *Geophysical Research Letters*, vol. 43, pp. 4189–4196, 2016.
- [24] A. R. Gusman, Y. Tanioka, B. T. MacInnes, and H. Tsushima, "A methodology for near-field tsunami inundation forecasting: Application to the 2011 Tohoku tsunami: Tsunami inundation forecasting method," *Journal of Geophysical Research: Solid Earth*, vol. 119, no. 11, pp. 8186–8206, 2014.
- [25] Y. Hayashi, H. Tsushima, K. Hirata, K. Kimura, and K. Maeda, "Tsunami source area of the 2011 off the Pacific coast of Tohoku Earthquake determined from tsunami arrival times at offshore observation stations," *Earth, Planets and Space*, vol. 63, no. 7, p. 54, 2011.
- [26] M. Heesemann, T. L. Insua, M. Scherwath, K. S. Juniper, and K. Moran, "Ocean Networks Canada: From Geohazards Research Laboratories to Smart Ocean Systems," *Oceanography*, vol. 27, no. 2, pp. 151–153, 2014. [Online]. Available: <http://www.jstor.org/stable/24862165>
- [27] G. Hendin and M. Stiassnie, "Tsunami and acoustic-gravity waves in water of constant depth," *Physics of Fluids*, vol. 25, no. 8, p. 086103, 2013.
- [28] M. Hoshiba and T. Ozaki, "Earthquake early warning and tsunami warning of the Japan Meteorological Agency, and their performance in the 2011 off the Pacific Coast of Tohoku Earthquake," in *Early Warning for Geological Disasters*, ser. Advanced Technologies in Earth Sciences, F. Wenzel and J. Zschau, Eds. Springer Berlin Heidelberg, 2014, pp. 1–28. [Online]. Available: [http://dx.doi.org/10.1007/978-3-642-12233-0\\_1](http://dx.doi.org/10.1007/978-3-642-12233-0_1)
- [29] H. Kanamori, "Mechanism of Tsunami Earthquakes," *Physics of the Earth and Planetary Interiors*, vol. 6, no. 5, pp. 346–359, 1972.
- [30] H. Kanamori and M. Kikuchi, "The 1992 Nicaragua earthquake: A slow tsunami earthquake associated with subducted sediments," *Nature*, vol. 361, no. 6414, pp. 714–716, 1993.
- [31] T. Kanazawa, "Japan Trench earthquake and tsunami monitoring network of cable-linked 150 ocean bottom observatories and its impact to earth disaster science," *Underwater Technology Symposium*, pp. 1–5, 2013.
- [32] T. Kanazawa, K. Uehira, M. Mochizuki, T. Shinbo, H. Fujimoto, S. Noguchi, T. Kunugi, K. Shiomi, S. Aoi, T. Matsumoto *et al.*, "S-NET Project, cabled observation network for earthquakes and tsunamis," *SubOptic*, 2016.
- [33] Y. Kaneda, "The advanced ocean floor real time monitoring system for mega thrust earthquakes and tsunamis - application of DONET and DONET2 data to seismological research and disaster mitigation," *OCEANS 2016 MTS/IEEE Seattle*, 2010, pp. 1–6.
- [34] M. D. Kohler, E. S. Cochran, D. Given, S. Guiwits, D. Neuhauser, I. Henson, R. Hartog, P. Bodin, V. Kress, S. Thompson *et al.*, "Earthquake early warning ShakeAlert system: West coast wide production prototype," *Seismological Research Letters*, vol. 89, no. 1, pp. 99–107, 2017.
- [35] J. E. Kozdon and E. M. Dunham, "Constraining shallow slip and tsunami excitation in megathrust ruptures using seismic and ocean acoustic waves recorded on ocean-bottom sensor networks," *Earth and Planetary Science Letters*, vol. 396, pp. 56–65, 2014.
- [36] L. J. Leonard, C. A. Currie, S. Mazzotti, and R. D. Hyndman, "Rupture area and displacement of past Cascadia great earthquakes from coastal coseismic subsidence," *GSA Bulletin*, vol. 122, no. 11-12, pp. 2079–2096, 2010.
- [37] R. J. LeVeque, C. J. Vogl, and M. J. Berger, "On the relation between hydroacoustic and gravity waves in a compressible ocean," in preparation, 2018.
- [38] B. W. Levin and M. A. Nosov, *Physics of Tsunamis*, 2nd ed. Springer, 2016.
- [39] W. Li, "Analysis of Pressure Variations Observed at the Ocean Bottom during the 2003 Tokachi-Oki Earthquake," MS Thesis, Oregon State University, 2006. [Online]. Available: [https://ir.library.oregonstate.edu/concern/graduate\\_thesis\\_or\\_dissertations/9019s565g](https://ir.library.oregonstate.edu/concern/graduate_thesis_or_dissertations/9019s565g)
- [40] W. Li, H. Yeh, K. Hirata, and T. Baba, "Ocean-bottom pressure variations during the 2003 Tokachi-Oki earthquake," in *Nonlinear Wave Dynamics*. WORLD SCIENTIFIC, 2009, pp. 109–126.
- [41] B. Lipa, J. Isaacson, B. Nyden, and D. Barrick, "Tsunami arrival detection with high frequency (HF) radar," *Remote Sensing*, vol. 4, no. 5, pp. 1448–1461, 2012.
- [42] B. J. Lipa, D. E. Barrick, J. Bourq, and B. B. Nyden, "HF radar detection of tsunamis," *Journal of Oceanography*, vol. 62, no. 5, pp. 705–716, 2006.
- [43] T. Maeda, K. Obara, M. Shinohara, T. Kanazawa, and K. Uehira, "Successive estimation of a tsunami wavefield without earthquake source data: A data assimilation approach toward real-time tsunami forecasting," *Geophysical Research Letters*, vol. 42, pp. 7923–7932, 2015.
- [44] D. G. Masson, C. B. Harbitz, R. B. Wynn, G. Pedersen, and F. Løvholt, "Submarine landslides: Processes, triggers and hazard prediction," *Philosophical Transactions of the Royal Society A: Mathematical, Physical and Engineering Sciences*, vol. 364, no. 1845, p. 2009, 2006.
- [45] H. Matsumoto, S. Inoue, and T. Ohmachi, "Some features of water pressure change during the 2011 Tohoku earthquake," *Proceedings of the International Symposium on Engineering Lessons Learned from the 2011 Great East Japan Earthquake*, 2012.
- [46] D. Melgar, R. M. Allen, S. Riquelme, J. Geng, F. Bravo, J. C. Baez, H. Parra, S. Barrientos, P. Fang, Y. Bock, M. Bevis, D. J. Caccamise, C. Vigny, M. Moreno, and R. Smalley, "Local tsunami warnings:

- Perspectives from recent large events,” *Geophysical Research Letters*, vol. 43, no. 3, p. 2015GL067100, 2016.
- [47] D. Melgar, B. W. Crowell, J. Geng, R. M. Allen, Y. Bock, S. Riquelme, E. M. Hill, M. Protti, and A. Ganas, “Earthquake magnitude calculation without saturation from the scaling of peak ground displacement,” *Geophysical Research Letters*, vol. 42, no. 13, pp. 5197–5205, 2015.
- [48] D. Melgar, R. J. LeVeque, D. S. Dreger, and R. M. Allen, “Kinematic rupture scenarios and synthetic displacement data: An example application to the Cascadia subduction zone,” *Journal of Geophysical Research: Solid Earth*, vol. 121, pp. 6658–6674, 2016.
- [49] R. L. Nigbor, “Six-degree-of-freedom ground-motion measurement,” *Bulletin of the Seismological Society of America*, vol. 84, no. 5, pp. 1665–1669, 1994.
- [50] NOAA Center for Tsunami Research, “DART (Deep-ocean Assessment and Reporting of Tsunamis).” [Online]. Available: <https://nctr.pmel.noaa.gov/Dart/>
- [51] M. A. Nosov, “Tsunami generation in compressible ocean,” *Physics and Chemistry of the Earth, Part B: Hydrology, Oceans and Atmosphere*, vol. 24, no. 5, pp. 437–441, 1999.
- [52] M. A. Nosov and S. V. Kolesov, “Elastic oscillations of water column in the 2003 Tokachi-oki tsunami source: In-situ measurements and 3-D numerical modelling,” *Nat. Hazards Earth Syst. Sci.*, vol. 7, no. 2, pp. 243–249, 2007.
- [53] T. Saito and H. Tsushima, “Synthesizing ocean bottom pressure records including seismic wave and tsunami contributions: Toward realistic tests of monitoring systems,” *Journal of Geophysical Research: Solid Earth*, vol. 121, no. 11, pp. 8175–8195, 2016.
- [54] V. Sardina, C. McCreery, and G. Fryer, “Compilation and analysis of two decades worth of tsunami bulletins issued by the Pacific Tsunami Warning Center,” *Proceedings of the 16th World Conference on Earthquake Engineering*, no. Paper No 193, pp. S–B1 463 015 136, 2017.
- [55] D. A. Schmidt, W. Wilcock, P. Bodin, F. González, M. Harrington, R. LeVeque, D. Manalang, E. Roland, and J. Vidale, “Offshore geophysical monitoring of Cascadia for early warning and hazards research,” Workshop Report, 2017. [Online]. Available: <http://cascadiaoffshore.org/story/Workshop.html>
- [56] L. M. Smith, J. A. Barth, D. S. Kelley, A. Plueddemann, I. Rodero, G. A. Ulses, M. F. Vardaro, and R. Weller, “The Ocean Observatories Initiative,” *Oceanography*, vol. 31, no. 1, pp. 16–35, 2018. [Online]. Available: <http://www.jstor.org/stable/26307783>
- [57] Y. Tanioka, “Tsunami simulation method assimilating ocean bottom pressure data near a tsunami source region,” *Pure and Applied Geophysics*, vol. 175, no. 2, pp. 721–729, 2018.
- [58] V. V. Titov, F. I. Gonzalez, E. N. Bernard, M. C. Eble, H. O. Mofjeld, J. C. Newman, and A. J. Venturato, “Real-time tsunami forecasting: Challenges and solutions,” *Nat Hazards*, vol. 35, no. 1, pp. 35–41, 2005.
- [59] M. Trifunac and M. Todorovska, “A note on the useable dynamic range of accelerographs recording translation,” *Soil dynamics and Earthquake engineering*, vol. 21, no. 4, pp. 275–286, 2001.
- [60] D. R. Toomey, R. M. Allen, A. H. Barclay, S. W. Bell, P. D. Bromirski, R. L. Carlson, X. Chen, J. A. Collins, R. P. Dziak, B. Evers, D. W. Forsyth, P. Gerstoft, E. E. E. Hooft, D. Livelybrooks, J. A. Lodewyk, D. S. Luther, J. J. McGuire, S. Y. Schwartz, M. Tolstoy, A. M. Tréhu, M. Weirathmueller, and W. S.D. Wilcock, “The Cascadia Initiative: A sea change in seismological studies of subduction zones.” *Oceanography*, vol. 27, no. 2, pp. 138–150, 2014.
- [61] C. J. Vogl and R. J. LeVeque, “A High-Resolution Finite Volume Seismic Model to Generate Seafloor Deformation for Tsunami Modeling,” *Journal of Scientific Computing*, vol. 73, no. 2-3, pp. 1204–1215, 2017.
- [62] L. M. Wallace, S. C. Webb, Y. Ito, K. Mochizuki, R. Hino, S. Henrys, S. Y. Schwartz, and A. F. Sheehan, “Slow slip near the trench at the Hikurangi subduction zone, New Zealand,” *Science*, vol. 352, no. 6286, pp. 701–704, 2016.
- [63] W. S. D. Wilcock, D. A. Schmidt, J. E. Vidale, M. J. Harrington, P. Bodin, G. S. Cram, J. R. Delaney, F. I. Gonzalez, D. S. Kelley, R. J. LeVeque, D. A. Manalang, C. McGuire, E. C. Roland, M. W. Stoermer, J. W. Tilley, and C. Vogl, “Designing an offshore geophysical network in the Pacific Northwest for earthquake and tsunami early warning and hazard research,” in *OCEANS 2016 MTS/IEEE Monterey*, 2016, pp. 1–8.
- [64] R. Wilson, P. Lynett, K. Miller, A. Admire, A. Aykut, E. Curtis, L. Dengler, M. Hornick, T. Nicolini, and D. Peterson, “Maritime Tsunami Response Playbooks: Background Information and Guidance for Response and Hazard Mitigation Use,” 2016,

California Geological Survey Special Report 241. [Online]. Available: [ftp://ftp.consrv.ca.gov/pub/dmg/pubs/sr/SR\\_241/CGS\\_SR241.pdf](ftp://ftp.consrv.ca.gov/pub/dmg/pubs/sr/SR_241/CGS_SR241.pdf)